

Guiding of vortices and ratchet effect in superconducting films with asymmetric pinning potential

Valerij A. Shklovskij*

*Institute of Theoretical Physics, National Science Center–Kharkov Institute of Physics and Technology, 61108 Kharkov, Ukraine
and Department of Physics, Kharkov National University, 61077 Kharkov, Ukraine*

Vladimir V. Sosedkin

Physical Department, Kharkov National University, 61077 Kharkov, Ukraine

(Received 21 July 2009; revised manuscript received 17 November 2009; published 21 December 2009)

Two-dimensional vortex dynamics in a ratchet washboard planar pinning potential in the presence of thermal fluctuations is considered on the basis of a Fokker-Planck equation. *Explicit* expressions for two nonlinear anisotropic voltages (longitudinal and transverse with respect to the current direction) are derived and analyzed. The physical origin of these odd (with respect to magnetic field or transport current direction reversal) voltages is caused by the interplay between the even effect of vortex guiding and the ratchet asymmetry. Both voltages are going to zero in the linear regimes of the vortex motion [i.e., in the thermally activated flux flow (TAFF) and Ohmic flux flow (FF) regimes] and have a bumplike current or temperature dependence in the vicinity of the highly nonlinear resistive transition from the TAFF to the FF.

DOI: [10.1103/PhysRevB.80.214526](https://doi.org/10.1103/PhysRevB.80.214526)

PACS number(s): 74.25.Qt, 74.25.Fy, 74.25.Sv, 74.40.+k

I. INTRODUCTION

Since last decade vortex ratchets, which exploit asymmetric vortex dynamics, have been attracting considerable attention.^{1–6} The common feature of superconducting ratchet systems is their rectifying property: the application of the alternating current to a superconductor patterned with a periodic asymmetric pinning potential can produce vortex motion whose direction is determined only by the asymmetry of the pattern. Although considerable theoretical work exists,¹ only few experiments have been realized. Recently a vortex lattice ratchet effect has been investigated in Nb films sputtered on arrays of nanometric Ni triangles, which produce the periodic asymmetric pinning potential.² Similar effects were also discussed for YBa₂Cu₃O_{7– δ} superconducting films with antidots.⁴ Earlier it has been proposed in Ref. 5 how the ratchet effect can be used to remove vortices from low-temperature superconductors.

Unfortunately, a full temperature-dependent theoretical description of the superconducting devices proposed in Refs. 2–5 is not available due to the complexity of the two-dimensional periodic pinning potential in Refs. 2–5 used. In particular, a theoretical explanation of the experimentally available study of the vortex flow along the vortex channeling directions in above-mentioned structures is a difficult problem. Due to this reason we propose below to study experimental ratchet properties of superconductors on the basis of a more simple ratchet device for which exists a full theoretical description (at least in the single-vortex approximation) of its two-dimensional vortex dynamics within the framework of a Fokker-Planck approach. The first communication on this subject has been published in Ref. 6.

It is noticeable that such a device has already been exploited many years ago by Morrison and Rose in their experiments on controlled asymmetric (as now we say “ratchet”) surface pinning in the superconducting-alloy films.⁷ Recent progress in the fabrication of submicrometric

structures with a periodic ratchet modulation of their thickness by methods of electron-beam lithography⁸ or molecular-beam epitaxy on faceted substrates⁹ allows us to prepare Nb films with a similar well-controlled asymmetric washboard pinning structure. Note also that the main feature of similar structures is the existence of well-defined *guiding* of vortices along the channels of the washboard pinning potential at relatively low temperatures.

One of the first experimental observations of guided vortex motion in the flux flow (FF) regime was made by Niessen and Weijsenfeld still in 1969.¹⁰ They studied guided vortex motion in the cold-rolled sheets of a Nb-Ta alloy by measuring transverse (T) voltages of the pattern for different magnetic fields H , transport current densities J , temperatures T , and different angles α between the rolling and current directions. The (H, J, T, α) dependences of the cotangent of the angle β between the average vortex velocity $\langle \mathbf{v} \rangle$ and the \mathbf{j} direction were presented. For the discussion, a simple theoretical model was suggested, based on the assumption that vortex pinning and guiding can be described in terms of an isotropic pinning force plus a pinning force with a fixed direction which was perpendicular to the rolling direction. The experimentally observed dependence of the transverse and longitudinal (L) voltages on the magnetic field *in the flux flow regime* as a function of the angle α was in agreement with this model. However, the dynamics of the vortex that is moving transverse to the pinning channels has substantially nonlinear behavior and cannot be entirely explained within the flux flow approach.

The *nonlinear guiding* problem was exactly solved at first only for washboard planar pinning potential (PPP) within the framework of the two-dimensional stochastic model of anisotropic pinning, which takes into account the vortex and the Hall viscosity coefficients and based on the Fokker-Planck equation with a concrete form of the symmetric pinning potential.^{11,12}

Rather simple formulas were derived in Ref. 12 for the

experimentally observable *nonlinear* even (+) and odd (−) (with respect to the magnetic field reversal) longitudinal and transverse magnetoresistivities $\rho_{\parallel,\perp}^{\pm}(j, t, \alpha, \epsilon)$ as functions of the dimensionless transport current density j , dimensionless temperature t , and relative volume fraction $0 < \epsilon < 1$ occupied by the parallel twin planes directed at an angle α with respect to the current direction. The $\rho_{\parallel,\perp}^{\pm}$ formulas were presented in Ref. 12 as linear combinations of the even and odd parts of the function $\nu(j, t, \alpha, \epsilon)$, which can be considered as the probability of overcoming the potential barrier of the pinning channel; this made it possible to give a simple physical treatment of the nonlinear regimes of vortex motion.

In addition to the appearance of a well-known relatively large even transverse ρ_{\perp}^{+} resistivity,¹⁰ generated by the guiding of vortices along the channels of the washboard PPP, explicit expressions for *two nonlinear anisotropic Hall resistivities* ρ_{\parallel}^{-} and ρ_{\perp}^{-} were derived and analyzed. The physical origin of these *odd* contributions caused by the subtle interplay between even effect of vortex guiding and the odd Hall effect. Both additional resistivities were going to zero in the linear regimes of the vortex motion [i.e., in the thermally activated flux flow (TAFF) and Ohmic FF regimes and had a bumplike current or temperature dependence in the vicinity of highly nonlinear resistive transition from the TAFF to the FF regimes]. As the odd resistivities arose due to the Hall effect, their characteristic scale was proportional to the small Hall constant as for ordinary odd Hall effect investigated earlier in Ref. 11.

In contrast to the model which uses the uniaxial symmetric PPP (Ref. 12) with the Hall effect, we consider below the simpler modified model with asymmetric (ratchet) sawtooth washboard pinning potential where the Hall effect is absent. It will be shown the appearance of two steplike and two bumplike singularities in the $\rho_{\parallel,\perp}^{+}$ and $\rho_{\parallel,\perp}^{-}$ (Hall-like) resistive responses in this model, even in the absence of the Hall effect.

The objective of this paper is to present results of a temperature-dependent theory for the calculation of the nonlinear magnetoresistivity tensor for asymmetric sawtooth washboard pinning potential at arbitrary value of asymmetry parameter $0 < \epsilon < 1$ for the case of in-plane geometry of experiment. This approach will give us the experimentally important theoretical model which demonstrates the $\rho_{\parallel,\perp}^{\pm}$ magnetoresistivities for all corresponding values of the modeling parameters and predicts an appearance of the nonlinear magnetoresistivity ρ_{\perp}^{-} at some sets of parameters ϵ (when the *Hall coefficient* is zero) due to the asymmetry of the washboard PPP.

The organization of the paper is as follows. Section II presents those general results in the stochastic model of anisotropic pinning which do not require specification of the form of the pinning potential: the Fokker-Planck method in the two-dimensional model of anisotropic pinning and the nonlinear resistivity and conductivity tensors. In Sec. III A we substitute a specific sawtooth form of the pinning potential into the general formulas of the preceding section. This enables us to find the *exact* analytical solution of our problem and to derive and analyze theoretically formulas for the resistive responses $\rho_{\parallel,\perp}^{\pm}(j, t, \alpha, \epsilon)$. Section III B is dedicated to an analysis of the nonlinear guiding effect in the presence

of the PPP asymmetry, and Sec. III C discusses the behavior of resistive responses due to the asymmetry of pinning potential. Section III D considers a magnetoresistivity stability with respect to small deviations of the angle α from its values adopted in the L and T geometries of experiment. Section III E gives a short discussion of main features for the cases of weak and strong asymmetries. Finally, Sec. IV presents the obtained results and formulates the conclusions.

II. GENERAL RESULTS

A. Fokker-Plank method in the anisotropic pinning model

The Langevin equation for a vortex moving with velocity \mathbf{v} in a magnetic field $\mathbf{B} = n\mathbf{B}$ ($B \equiv |\mathbf{B}|$, $\mathbf{n} = n\mathbf{z}$, \mathbf{z} is the unit vector in the z direction, and $n = \pm 1$) has the form

$$\eta\mathbf{v} = \mathbf{F}_L + \mathbf{F}_p + \mathbf{F}_{th}, \quad (1)$$

where $\mathbf{F}_L = n(\Phi_0/c)\mathbf{j} \times \mathbf{z}$ is the Lorentz force (Φ_0 is the magnetic flux quantum, c is the speed of light, and \mathbf{j} is the transport current density), $\mathbf{F}_p = -\nabla U_p(x)$ is the anisotropic pinning force ($U_p(x)$ is the uniaxial and asymmetric [$U_p(x) \neq U_p(-x)$] planar pinning potential), and η is the electronic viscosity constant. The thermal fluctuation force \mathbf{F}_{th} is represented by a Gaussian white noise, whose stochastic properties are assigned by the relations

$$\langle F_{th,i}(t) \rangle = 0, \quad \langle F_{th,i}(t) F_{th,j}(t') \rangle = 2T\eta\delta_{ij}\delta(t-t'), \quad (2)$$

where T is the temperature in energy units. Employing relations (2), we can reduce Eq. (1) to a system of Fokker-Planck equations as follows:

$$\frac{\partial P}{\partial t} = -\nabla \cdot \mathbf{S}, \quad (3)$$

$$\eta\mathbf{S} = (\mathbf{F}_L + \mathbf{F}_p)P - T\nabla P, \quad (4)$$

where $P = P(\mathbf{r}, t)$ is the probability density associated with finding the vortex at the point $\mathbf{r} = \mathbf{r}(x, y)$ at the time t , and

$$\mathbf{S}(\mathbf{r}, t) \equiv P(\mathbf{r}, t)\mathbf{v}(\mathbf{r}, t) \quad (5)$$

is the probability flux density of the vortex. Since the anisotropic pinning potential is assumed to depend only on the x coordinate and is assumed to be periodic [$U_p(x) = U_p(x+a)$, where a is the period], the pinning force is always directed along the x axis (with unit anisotropy vector \mathbf{x} ; see Fig. 2) so that it has no component along the y axis [$F_{py} = -dU_p(x)/dy = 0$]. Thus, Eq. (4) in the stationary case for the functions $P = P(x)$ and $\mathbf{S} = (S_x, S_y) = S_x(x)\mathbf{x} + S_y(x)\mathbf{y}$ reduces to the equations

$$\eta S_x = P(x) \left(F_{Lx} - \frac{dU_p}{dx} \right) - T \frac{dP}{dx}, \quad (6)$$

$$\eta S_y = P(x) F_{Ly}, \quad (7)$$

where $F_{Lx} = n(\Phi_0/c)j \cos \alpha$ and $F_{Ly} = -n(\Phi_0/c)j \sin \alpha$ are the x and y components of the Lorentz force, respectively, and α is the angle between the direction of the transport current density \mathbf{j} and the y axis (see Figs. 1 and 2). Invoking

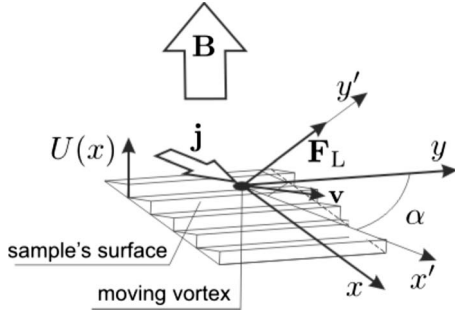


FIG. 1. Diagram of a superconductor in the presence of an external magnetic field \mathbf{B} . A direct transport current with density \mathbf{j} flowing along the x' direction induces a Lorentz force \mathbf{F}_L that acts along the y' direction. The superconductor is patterned with an asymmetric uniaxial planar pinning potential (asymmetric PPP) $U(x,y)=U(x) \neq U(-x)$, whose shape is shown in Fig. 3. The potential is periodic along the x axis and translational invariant along the y axis.

the condition of stationarity for Eq. (3) and eliminating S_y from Eqs. (6) and (7) we obtain

$$T \frac{dP}{dx} + \left(\frac{dU_p}{dx} - F_{Lx} \right) P = -S_x \eta. \quad (8)$$

From the mathematical point of view, Eq. (8) is the Fokker-Planck equation of the one-dimensional vortex dynamics. The solution of Eq. (8) for periodic boundary conditions $P(0)=P(a)$ and one-dimensional periodic pinning potential of general form is

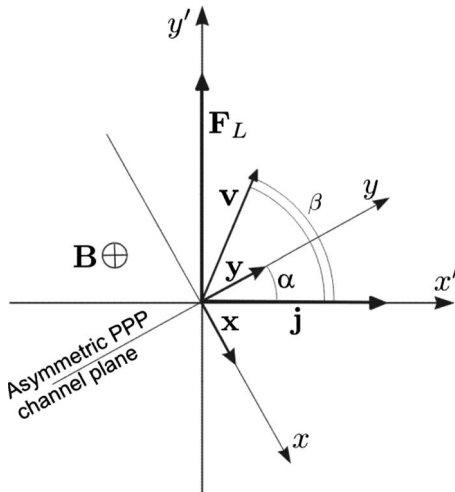


FIG. 2. System of coordinates xy (with the unit vectors \mathbf{x} and \mathbf{y}) associated with the asymmetric PPP (the unit vector \mathbf{y} points along the pinning channels) and the system of coordinates $x'y'$ associated with the direction of the transport current density vector \mathbf{j} , which points along the x' axis; α is the angle between the asymmetric PPP channels direction and the transport current density vector \mathbf{j} and β is the angle between the average velocity vector \mathbf{v} of the vortices and the transport current density vector \mathbf{j} ; \mathbf{F}_L is the Lorentz force.

$$P(x) = \frac{\eta S_x}{T} \frac{f(a)f(x)}{f(a)-f(0)} \int_x^{x+a} \frac{d\xi}{f(\xi)}, \quad (9)$$

where $f(\xi) = \exp\{[F_{Lx}\xi - U_p(\xi)]/T\}$.

Using the definition of the vortex mean velocity,

$$\langle \mathbf{v} \rangle = \int_0^a \mathbf{S}(x) dx / \int_0^a P(x) dx, \quad (10)$$

we obtain the expressions for the x and y components of the vortex mean velocity,

$$\langle v_x \rangle = \int_0^a S_x(x) dx / A = S_x a / A = F_{Lx} \nu(F_{Lx}) / \eta, \quad (11)$$

$$\langle v_y \rangle = \int_0^a S_y(x) dx / A = F_{Ly} / \eta, \quad (12)$$

where $A = \int_0^a P(x) dx$ and

$$\frac{1}{\nu(F_{Lx})} \equiv \frac{F_{Lx}}{Ta[1 - \exp(-F_{Lx}a/T)]} \int_0^a dx \int_0^a dx' \times \exp\left(-\frac{F_{Lx}x}{T}\right) \exp\left(\frac{U_p(x+x') - U_p(x')}{T}\right). \quad (13)$$

The dimensionless function $\nu(F_{Lx})$ in the limit $F_{Lx} \rightarrow 0$ coincides with the analogous quantity introduced in Ref. 11. It has the physical meaning of the probability of the vortex overcoming the potential barrier, the characteristic value of which we denote as U_0 . This can be seen by considering the limiting cases of high ($T \gg U_0$) and low ($T \ll U_0$) temperatures. In the case of high temperatures we have $\nu \approx 1$, and expression (13) corresponds to the FF regime. Indeed, in this case the influence of pinning can be neglected. In the case of low temperatures ν is a function of the transport current. For strong currents ($F_{Lx}a \gg U_0$) the potential barrier disappears, $\nu \approx 1$, and the FF regime is realized. For weak currents ($F_{Lx}a \ll U_0$) we have $\nu \sim \exp(-U_0/T)$, which corresponds to the TAFF regime. The transition from the TAFF regime to the FF regime is associated with a lowering of the potential barrier with growth of the current.

B. Nonlinear resistivity and conductivity tensors

The average electric field in the xy coordinate system induced by the moving vortices is given by

$$\mathbf{E} = (1/c)\mathbf{B} \times \langle \mathbf{v} \rangle = n(B/c)(-\langle v_y \rangle \mathbf{x} + \langle v_x \rangle \mathbf{y}). \quad (14)$$

Taking Eqs. (11), (12), and (14) we obtain the dimensionless magnetoresistivity tensor $\hat{\rho}$ (having components measured in units of the flux flow resistivity ρ_f) for the nonlinear law $\mathbf{E} = \hat{\rho}(j)\mathbf{j}$,

$$\hat{\rho} = \begin{pmatrix} \rho_{xx} & \rho_{xy} \\ \rho_{yx} & \rho_{yy} \end{pmatrix} = \begin{pmatrix} 1 & 0 \\ 0 & \nu(f) \end{pmatrix}, \quad (15)$$

where the dimensionless components of the electric field are measured in units of $E_0 = BU_0/ca\eta$, and of the current, in units of $j_0 = cU_0/\Phi_0 b$, and

$$f = -\frac{F_{Lx}b}{U_0} = mnj_y = mnj \cos \alpha = pj \cos \alpha, \quad (16)$$

where $m = \pm 1$ determines the transport current reversal ($j = |\mathbf{j}|$), $n = \pm 1$ determines the magnetic field direction reversal ($\mathbf{B} = n|\mathbf{B}|$), $p = mn$ is the combination for simplification of the current and magnetic field direction reversal, and α is the angle between the current direction and asymmetric PPP channels.

The conductivity tensor $\hat{\sigma}$ (the components of which are measured in units of $1/\rho_f$), which is the inverse tensor to $\hat{\rho}$, has the form

$$\hat{\sigma} = \begin{pmatrix} \sigma_{xx} & \sigma_{xy} \\ \sigma_{yx} & \sigma_{yy} \end{pmatrix} = \begin{pmatrix} 1 & 0 \\ 0 & \nu^{-1}(f) \end{pmatrix}. \quad (17)$$

From Eqs. (15) and (17) we see that off-diagonal components of the $\hat{\rho}$ and $\hat{\sigma}$ tensors are zero, and the nonlinear components of the $\hat{\rho}$ and $\hat{\sigma}$ tensors are functions of the external force value f through the external current density \mathbf{j} , the temperature T , and the angle α .

The experimentally measurable resistive responses refer to a coordinate system tied to the current (see Fig. 2). The longitudinal and transverse (with respect to the current direction) components of the electric field, E_{\parallel} and E_{\perp} , are related to E_x and E_y by the simple expressions

$$\begin{aligned} E_{\parallel} &= E_x \sin \alpha + E_y \cos \alpha, \\ E_{\perp} &= -E_x \cos \alpha + E_y \sin \alpha. \end{aligned} \quad (18)$$

Then according to Eqs. (15) and (18), the expressions for the experimentally observable longitudinal and transverse (with respect to the \mathbf{j} direction) magnetoresistivities $\rho_{\parallel} \equiv E_{\parallel}/j$ and $\rho_{\perp} \equiv E_{\perp}/j$ have the form

$$\begin{aligned} \rho_{\parallel} &= \sin^2 \alpha + \nu(f) \cos^2 \alpha, \\ \rho_{\perp} &= [\nu(f) - 1] \cos \alpha \sin \alpha. \end{aligned} \quad (19)$$

We introduce the L and T geometries in which $\mathbf{j} \parallel \mathbf{x}$ and $\mathbf{j} \perp \mathbf{x}$, respectively. From Eq. (19) it follows that in the L geometry vortex motion takes place along the pinning channels (the guiding effect), and in the T geometry it is transverse to the pinning channels direction (the slipping effect). In the L geometry the critical current is equal to zero since the FF regime is realized for guided vortex motion along pinning channels direction. In the T geometry, i.e., for the vortex motion transverse to the pinning channels, a pronounced nonlinear regime is realized for $T \ll U_0$, in the range $j_{cr1} < j < j_{cr2}$, the onset of which corresponds (depending on the sign of m) to the one of two crossover currents $j = j_{cr1}$ or $j = j_{cr2}$; and for $T \geq 0$ we have $j_{cr1,2} \approx j_{c1,2}$, where $j_{c1,2}$ are two critical currents at $T=0$ in opposite directions. It is evident that the presence of different crossover currents for mutually opposite directions along the vector \mathbf{x} is a direct consequence of an asymmetric pinning potential.

Let us consider a diagram of the dynamical states of the vortex system in the (j_x, j_y) plane for $T \ll U_0$ (Fig. 4). For arbitrary angle α the tip of the vector \mathbf{j} can lie in two different regions which are different in their physical meanings. If

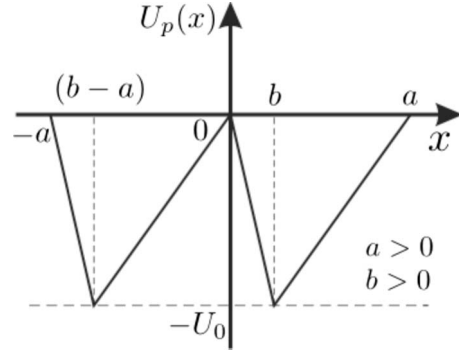


FIG. 3. Asymmetric sawtooth pinning potential $U_p(x)$: a is the potential period (width of the potential channels), b is the x coordinate of the minimum of the potential well, and U_0 is the depth of the potential well.

$j_y < j_{cr1}$ or $j_y < j_{cr2}$ the guided vortex motion takes place (the guiding region). For $j_y > j_{cr1}$ or $j_y < j_{cr2}$ the guided motion along the pinning channels is joined by motion transverse to the pinning channels (the slipping region). It is clear that if we apply an alternating harmonic current j^{ac} such that an amplitude of the current along the y axis satisfies to the relation $j_{cr1} < j_y^{ac} < j_{cr2}$, it will lead to a motion of vortices along the x axis as they can overcome a pinning potential only in one direction. It is the occurrence of the ratchet effect.

III. VORTEX PINNING ON ASYMMETRIC PPP AND ANALYSIS OF NONLINEAR REGIMES

A. Pinning potential and ν -function behavior

The nonlinear properties of the resistivity tensor $\hat{\rho}$, as can be seen from formula (15), are completely determined by the

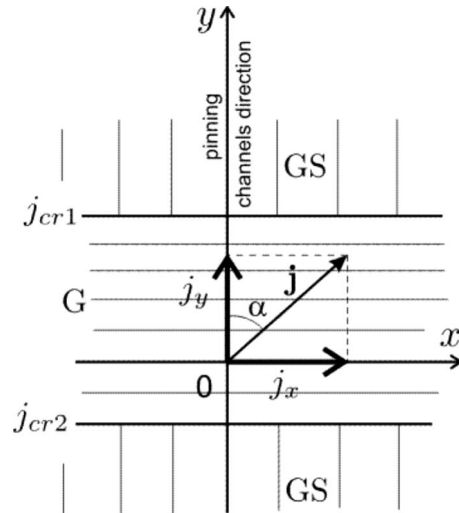


FIG. 4. Diagram of dynamic states of the vortex system in the xy plane for $T \ll U_0$; G is the region of motion of the vortices along the pinning channels (the guiding effect) and GS is the region of motion of the vortices along and transverse to the pinning channels (the guiding and slipping effects together); j_{cr1} and j_{cr2} are the crossover currents for mutually opposite directions along the vector \mathbf{y} corresponding to a transition from region G to region GS when the j_y is increasing.

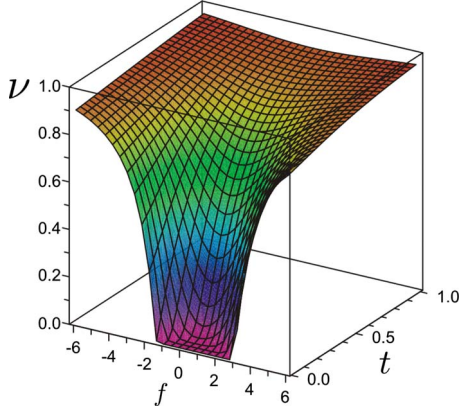


FIG. 5. (Color online) The dependence $\nu(f, t)$ for fixed value of the asymmetry parameter $\varepsilon_0=1/3$.

behavior of the function ν , which has the physical sense of the probability of a vortex overcoming the potential barriers created by the channels of asymmetric pinning potential. In turn, the function ν , according to formula (13), depends on the form of the pinning potential. Above we considered the simplest case of the asymmetric PPP that has sawtoothlike form (see Fig. 3),

$$U_p(x) = \begin{cases} -F_{p1}x, & 0 \leq x < b \\ -F_{p2}(x-a), & b < x \leq a, \end{cases} \quad (20)$$

where $F_{p1}=U_0/b$ and $F_{p2}=U_0/(b-a)$ are the pinning forces in the different directions of the x axis and U_0 is the depth of a potential well, a is the period of the asymmetric PPP ($a \geq b$), and $\varepsilon=b/a$ is the parameter characterizing the asymmetry of the pinning potential ($0 < \varepsilon < 1$ and $\varepsilon=1/2$ corresponds to the symmetric well).

Substituting the potential (20) into formula (13) for the probability function ν gives the following expressions:

$$\nu(f, t, \varepsilon) = [f(\varepsilon - 1) - 1]^2 (f\varepsilon - 1)^2 / [f(A + B)],$$

$$A = f[f\varepsilon(\varepsilon - 1) + 1]^2 + (1 - \varepsilon)(2f\varepsilon - 1)^2 + \varepsilon[f(\varepsilon - 1) - 1],$$

$$B = t\{\cosh[(f\varepsilon - 1 - f/2)/t] - \cosh[f/(2t)]\} / \sinh[f/(2t)], \quad (21)$$

where $f=-F_{Lx}a/U_0$ is the dimensionless external force which gives the ratio of this force to the average pinning force U_0/a and $t=T/U_0$ is the dimensionless temperature which gives the ratio of the energy of the thermal fluctuations of the vortices to the depth of the potential wells U_0 . In our case the dimensionless external force f also coincides (up to a sign) with the dimensionless transport current j_y , which is given by formula (16). At function evaluation (21) we assumed that the asymmetry parameter ε changes from zero value that corresponds to shift of the pinning potential minimum to the left, up to unity value that corresponds to shift of the potential minimum to the right and that naturally leads to as much as possible asymmetry of the pinning potential in the appropriate direction.

Let us consider now the dependence of the probability function $\nu(f, t, \varepsilon)$ on each of the quantities f , t , and ε for the

remaining quantities held fixed (denoted by the subscript “0”). The dependence $\nu(f, t) = \nu(f, t, \varepsilon_0)$ (see Fig. 5) shows ν as a function of the external force acting on a vortex at different temperatures and for constant asymmetry parameter value. The influence of the external force f acting on the vortices is that it lowers the height of the potential barrier for vortices localized along the channels of the asymmetric PPP and, consequently, increases the probability of escape from them. Raising the temperature also increases the probability that a vortex will escape from a potential well through an increase in the energy of the thermal fluctuations of the vortices. Thus, the pinning potential, leading as $f, t \rightarrow 0$ to localization of vortices, can be suppressed both by an external force and by an increase in the temperature. From Eq. (21) follows that

$$\lim_{t \rightarrow \infty} \nu(f, t, \varepsilon) = \lim_{f \rightarrow \infty} \nu(f, t, \varepsilon) = 1. \quad (22)$$

The function

$$\nu_0(f, \varepsilon) = \lim_{t \rightarrow 0} \nu(f, t, \varepsilon)$$

is equal to

$$\nu_0(f, \varepsilon) = \begin{cases} 0, & \frac{1}{\varepsilon - 1} < f < \frac{1}{\varepsilon} \\ \frac{(f\varepsilon - f - 1)(f\varepsilon - 1)}{f(f\varepsilon^2 - f\varepsilon - 2\varepsilon + 1)}, & \left(f < \frac{1}{\varepsilon - 1}\right) \cup \left(f > \frac{1}{\varepsilon}\right), \end{cases} \quad (23)$$

and corresponds to the zero-temperature limit.

From Eqs. (23) and (16) it follows that the crossover transport current and, respectively, crossover external force (in the dimensionless units) in both directions are $f_{cr1}=j_{cr1}=1/(\varepsilon-1)$ and $f_{cr2}=j_{cr2}=1/\varepsilon$ (see also the diagram of dynamic states in Fig. 4). If $0 < \varepsilon < 1/2$, then $|j_{cr1}| < |j_{cr2}|$, and for $1/2 < \varepsilon < 1$ we have $|j_{cr1}| > |j_{cr2}|$. Let us note also that the value $\varepsilon=1/3$, which we use in some figures of this paper, corresponds to the case when $j_{cr1}=2j_{cr2}$.

In the zero-temperature limit, for $|j_y| < |j_{cr1}|$, $|j_{cr2}|$ the vortices are trapped in the potential wells of the pinning channels and they cannot move across pinning barriers, while for $|j_y| > |j_{cr1}|$, $|j_{cr2}|$ the potential barrier disappears and the vortices begin to move in the one or both directions. Indicated inequalities divide (f, ε) plane into two regions: the first one is the full guiding region, where $\nu=0$, whereas in the second region $\nu \neq 0$ and vortices can move in the nonlinear resistive regimes.

It is easy to understand the influence of the temperature on the qualitative form of $\nu(j_y, \varepsilon)$. Specifically at low temperatures ($T \ll U_0$) a nonlinear transition takes place from the TAFF regime of vortex motion perpendicular to the pinning channels to the FF regime with growth of the external force, wherein the function $\nu(j_y, \varepsilon_0)$ has a characteristic nonlinear shape (see Fig. 5). At high temperatures ($T \gg U_0$) the FF regime is realized over the entire range of variation of the external current. At nonzero temperature j_{cr1} and j_{cr2} disappear at relatively high temperature because increasing of the

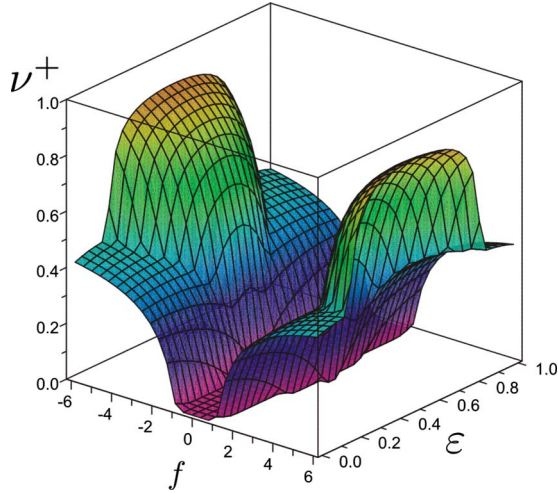


FIG. 6. (Color online) The dependence $\nu^+(f, \varepsilon)$ for fixed value of the temperature $t_0=0.05$.

temperature leads to smoothing of the function $\nu(j_y, \varepsilon)$ which in the limit $t \rightarrow \infty$ it simply degenerates in the plane $\nu(j_y, \varepsilon) = 1$ that corresponds to the free motion of the vortices.

In the limit $f \rightarrow 0$ we have

$$\nu_0(t, \varepsilon) = \frac{\exp(1/t)}{t^2[\exp(1/t) - 1]^2}. \quad (24)$$

From Eq. (24) it follows that, if the temperature is nonzero, the vortices can move at arbitrary small external force. This is in agreement with the explanation at the end of Sec. II A. Note that the value of $\nu_0(t, \varepsilon)$ does not depend on the parameter of asymmetry of a pinning potential.

As follows from Eqs. (16), (19), and (21) the dynamics of a vortex system depends substantially on the reversal of the directions of the current flow and the magnetic field. According to Eq. (16), the reversal of m and n signs equally cause the reversal of the Lorentz force F_L which changes the magnitude of the $\nu(f, t, \varepsilon)$ function due to the inversion of f . In order to consider only p -independent magnitudes of the ρ_{\parallel} and ρ_{\perp} resistivities in Eq. (19), we should introduce the even (+) and odd (-) magnetoresistivities with respect to the p inversion ($\rho(p)^{\pm} \equiv [\rho(p) \pm \rho(-p)]/2$). From this point of view it follows that we should present the function $\nu(f)$ as a sum of the even (+) and odd (-) parts with respect to inversion of the moving force,

$$\nu(p) = \nu^+(p) + \nu^-(p), \quad (25)$$

$$\nu^{\pm}(p) = \frac{\nu(pf, t, \varepsilon) \pm \nu(-pf, t, \varepsilon)}{2}, \quad (26)$$

where ν^{\pm} are even and odd parts of the ν function, respectively.

The most important features of the ν^{\pm} functions follow from Eqs. (22) and (26). As can be shown, the dependence $\nu^+(f, t)$ in the limiting cases is closely similar to the $\nu(f, t)$. Namely, the qualitative behavior and the limits of the component $\nu^+(f, t)$ as $f, t \rightarrow 0, \infty$ coincide with the corresponding limits of $\nu(f, t)$. The ν^- function has more sophisticated be-

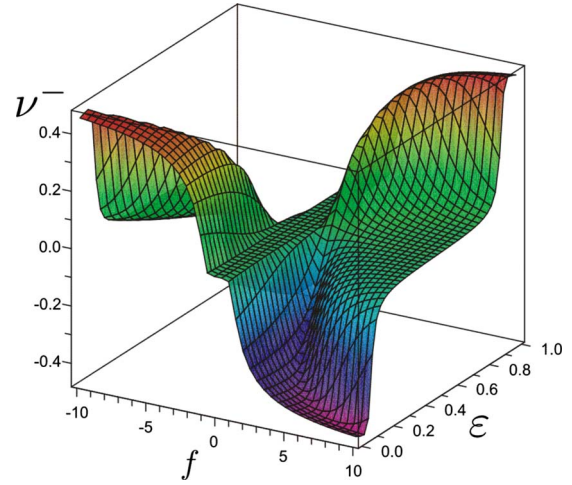


FIG. 7. (Color online) The dependence $\nu^-(f, \varepsilon)$ for fixed value of the temperature $t_0=0.05$.

havior, but if $f \rightarrow 0, \infty$ or $t \rightarrow \infty$, then ν^- tends to zero.

Now let us consider the $\nu^+(f, \varepsilon)$ behavior in more detail. It is easy to see in Fig. 6 that $\nu^+(f, \varepsilon)$ is always positive and symmetric about $f=0$ and $\varepsilon=1/2$ planes. Note also that at comparatively low temperatures ($t \ll 1$) the asymmetry parameter ε influences on the shape of the ν^+ function (see Fig. 6). Namely, in Fig. 6 we see the specific bumplike behavior of $\nu^+(\varepsilon)$ at $f > f_{cr1}, f_{cr2}$ and in this connection it should be pointed out that the magnitude of $\nu^+(f)$ for large values of f in the case of strong asymmetry (when ε is near 0 or 1) does not exceed 1/2.

Now we pass to a discussion of the $\nu^-(f, t, \varepsilon)$ graphs. Let us begin with considering the $\nu^-(f, \varepsilon)$ and $\nu^-(t, \varepsilon)$ functions taken at constant t and f , respectively (see Figs. 7 and 9). The graph of $\nu^-(f, \varepsilon)$ is antisymmetric about $f=0$, $\nu^-=0$, and $\varepsilon=1/2$ planes due to oddness of this function, whereas the $\nu^-(t, \varepsilon)$ graph is antisymmetric about $\varepsilon=1/2$ and $\nu^-=0$ planes.

As has been stated above, $\nu^-(f, t)$ tends to zero in the linear regimes and is nonzero in the region of nonlinearity of ν (see Fig. 8). It means that $\nu^-(f, t)$ can be suppressed with

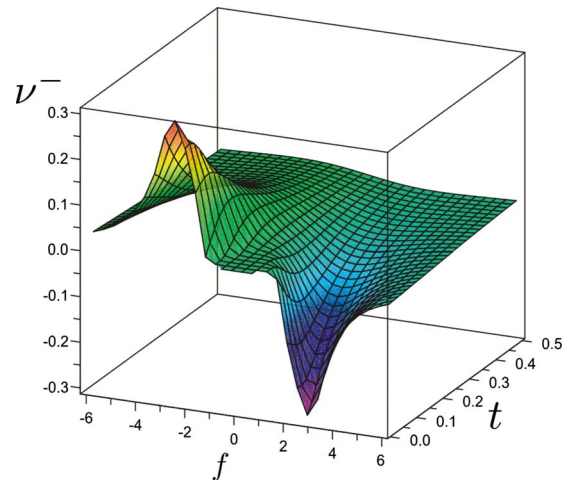


FIG. 8. (Color online) The dependence $\nu^-(f, t)$ for fixed value of the asymmetry parameter $\varepsilon_0=1/3$.

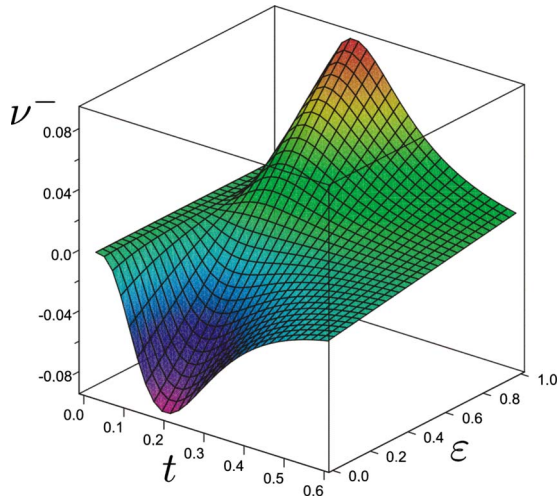


FIG. 9. (Color online) The dependence $\nu^-(t, \epsilon)$ for fixed value of the external motive force $f_0=0.7$.

increasing of the external motive force or temperature. When the value of temperature grows, the function $\nu^-(f, t)$ tends to zero since the temperature fluctuations at $t \gg 1$ in a superconductor suppress the influence of the pinning potential and the vortex; thus, it can move freely in any direction (the FF regime is realized). At small temperature, when the contribution of pinning potential is comparable or more than the contribution of temperature fluctuations ($t \ll 1$), the ν^- behavior is explained by interplay between the external motive force f and asymmetry of the pinning potential (which causes the appearance of the crossover currents $j_{cr1, cr2}$). If $f \ll f_{cr1}$, f_{cr2} and the temperature value is close to zero, then $\nu^-(f, t)$ also is close to zero because the vortex cannot move across pinning channels in any direction. When $f_{cr1} < f < f_{cr2}$ (or vice versa $f_{cr2} < f < f_{cr1}$ that depends on the value of the asymmetry parameter ϵ), then the TAFF regime is realized and the curve $\nu^-(f, t)$ accepts a bumplike form (see Fig. 8). In this case the ratchet effect occurs and vortices start to move in a direction that associated with the minimal pinning force. At strong external motive force, when $f \gg f_{cr1}$, f_{cr2} , the function $\nu^-(f)$ is also vanishing because external current suppresses influence of the pinning potential on the vortex (FF regime arises) as it follows from the general properties of the $\nu(f)$ function, and the vortices can freely move in any direction across the pinning channels. The width of the peak of a bumplike curve is associated with the value of asymmetry parameter ϵ and also can be simply presented as $2\Delta f_{cr} = 2||f_{cr1} - f_{cr2}|| = (|\epsilon| - |\epsilon - 1|) / [(\epsilon - 1)\epsilon]$. It means that, when $\epsilon \rightarrow 0, 1$, the width of the peak will tend to infinity and in Fig. 7 we see a change from the bumplike to the steplike dependence of $\nu^-(f)$. The maximum of the $\nu^-(f)$ function with respect to the external motive force f (see Figs. 7 and 8) corresponds to the maximum pinning force for both f_{cr1} and f_{cr2} , respectively.

The appearance of ν^- is a direct consequence of asymmetry of the pinning potential. When the asymmetry parameter ϵ is not equal to 1/2, then the same absolute value of a motive force applied in mutually opposite directions leads to different values of the function ν that leads to the occurrence of an odd component ν^- .

When the pinning potential is symmetric ($\epsilon=1/2$), the function ν^- is equal to zero (see Figs. 7 and 9). Also, for $\epsilon=1/2$ we regain the results of Ref. 13,

$$\nu(f, t, 1/2) = (u^2 - 1)^2 / \{u^2(u^2 - 1)2uf[\cosh(u/t) - \cosh(1/t)]/\sinh(u/t)\}, \quad (27)$$

where $u=f/2$.

Now we will obtain expressions from formulas (19) and (26) for the experimentally observed longitudinal and transverse resistivities (relative to the current direction) with the asymmetric pinning potential taken into account. We separate out their even and odd components relative to the current direction,

$$\rho_{\parallel}^+ = \nu^+ \cos^2 \alpha + \sin^2 \alpha, \quad (28)$$

$$\rho_{\perp}^+ = (\nu^+ - 1)\sin(2\alpha)/2, \quad (29)$$

$$\rho_{\perp}^- = \nu^- \sin(2\alpha)/2, \quad (30)$$

$$\rho_{\parallel}^- = \nu^- \cos^2 \alpha, \quad (31)$$

where ν^{\pm} are the above-defined even and odd components relative to the current direction of the function $\nu(f, t, \epsilon)$. In formulas (28) and (29) the nonlinear and linear terms separate out in a natural way. The physical reason for the appearance of linear terms is that in the model under consideration for $\alpha=\pi/2$ there is always a FF regime of vortex motion along the pinning channels.

In Ref. 12 the influence of the Hall effect on the occurrence of ν^- in the presence of symmetric pinning potential has been discussed. It has been shown that if the Hall constant is distinct from zero then ν^- is distinct from zero too, and vice versa. Now we see that the asymmetric PPP leads to the occurrence of an odd component $\nu^-(f)$ if we neglect the Hall effect. In order to estimate the influence of the Hall effect on the ρ_{\perp}^- response in the presence of the asymmetric pinning potential, and then to explain the way in which the Hall and asymmetric odd transverse responses should be separated experimentally, we considered this problem in the Appendix.

B. Peculiarities of nonlinear guiding effect in presence of the PPP asymmetry

As is well known,¹⁰ the specifics of anisotropic pinning consist of the noncoincidence of the directions of the external motive force acting on the vortex, and its velocity. In the presence of uniaxial PPP the pinning force in a superconductor is anisotropic: it is directed in the transverse direction with respect to the pinning channels and so is zero in the longitudinal direction. The most specific manifestation of such a pinning anisotropy are effects associated with the directed motion of vortices along the washboard channels, the so-called guided vortex motion or guiding, when the vortices tend to move along the pinning channels even if the external force acting on them is not aligned parallel to this channels. Another important feature of pinning anisotropy is that the longitudinal ρ_{\parallel}^+ and transverse ρ_{\perp}^+ magnetoresistivities of the

sample depend on substantially not only the temperature, but also on the angle α with which the vector \mathbf{j} intersects the pinning channels.

In order to describe the guided vortex motion along the pinning channels in the absence of the PPP asymmetry, the angle β between the transport current direction and vortex velocity can be used (see Fig. 2) and it can be shown that $\cot \beta = -\rho_{\perp}^{+} / \rho_{\parallel}^{+}$.

From Fig. 2 and from Eqs. (14) and (19) follows the formula

$$\begin{aligned} \beta &= \beta(j, t, \varepsilon, \alpha) = \operatorname{arccot}(\rho_{\perp} / \rho_{\parallel}) \\ &= \operatorname{arccot}\{[1 - \nu(j \cos \alpha, t, \varepsilon)] / [\tan \alpha \\ &\quad + \nu(j \cos \alpha, t, \varepsilon) \cot \alpha]\}, \end{aligned} \quad (32)$$

which is used to describe the guiding effect in the presence of asymmetry of the PPP. The guiding effect is expressed that much more strongly, the larger is the difference in directions of \mathbf{F}_L and \mathbf{v} , i.e., the smaller is the angle β . If $\beta = \alpha$, it means that a full guided motion of vortices exists when all vortices move parallel to the pinning channels and, on the contrary, if $\beta = \pi/2$, the free vortex motion exists (in the FF regime). We see from Eq. (32) that due to the presence of the PPP asymmetry the magnitude of the angle β depends on the sign of m , i.e., on the inversion of the direction of the vector \mathbf{j} . Only at $\varepsilon = 1/2$ this dependence is absent. Although the guiding effect conception is very important above all as illustration of directed vortex motion we should underline that guiding of the vortices is the necessary condition for the appearance of the *transversal* ratchet effect, while the value of the effect entirely depends on the distinction between probability of the vortices overcoming over pinning potential barriers in opposite directions as it follows from Sec. III. So the main peculiarities of the guided vortex motion which appear due to presence of the PPP asymmetry are the dependence of the guiding angle β on the inversion of the transport current direction and the appearance of the transversal ratchet effect.

C. Resistive responses due to asymmetry of the pinning potential

In this section we consider peculiarities of the resistive characteristics in the investigated model due to the asymmetry of the pinning potential. Experimentally, two types of measurements of the observed resistive characteristics are possible in a prescribed geometry defined by a fixed value of the angle α : current-voltage characteristic and resistive measurements, which investigate the dependence of the observed resistivities on the current density at a fixed temperature $\rho_{\parallel, \perp}^{\pm}(j, t_0)$ and on the temperature for fixed current density $\rho_{\parallel, \perp}^{\pm}(j_0, t)$. The form of these dependences is governed by a geometrical factor—the angle α between the directions of the current density vector \mathbf{j} and the PPP channels. There are two different forms of the dependence of $\rho_{\parallel, \perp}^{\pm}$ on the angle α [see formulas (28)–(31)]. The first of these is the “tensor” dependence, also present in the linear regimes (TAFF and FF regimes), which is external to the function ν . The second is through the dependence of the function ν on its argument $f = p j_y = p |\mathbf{j}| \cos \alpha$, which in the region of the transition from

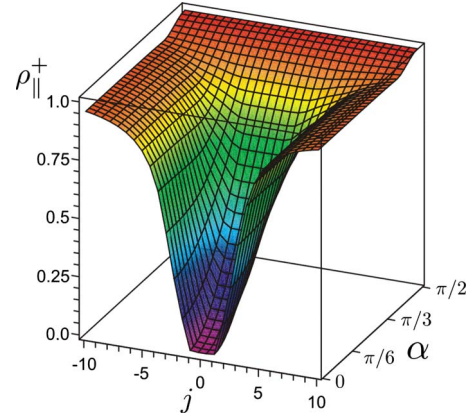


FIG. 10. (Color online) The dependence $\rho_{\parallel}^{+}(j, \alpha)$ for fixed value of the temperature $t_0 = 0.05$ and asymmetry parameter $\varepsilon_0 = 1/3$.

the TAFF to the FF regime is substantially nonlinear [see Eq. (21)].

First recall that in the absence of an asymmetry of the pinning potential ($\varepsilon = 1/2$) there exist only even resistivities $\rho_{\parallel, \perp}^{+}$ in the magnetic field, whereas the odd resistivities $\rho_{\parallel, \perp}^{-}$ are zero [see formulas (28)–(31)]. The presence of $\varepsilon \neq 1/2$ leads to the appearance of the odd component ν^{-} , which has a maximum in the region of the nonlinear transition from the TAFF to the FF regime and is essentially equal to zero outside this transitional region (see Figs. 7 and 9).

Let us analyze the resistive dependences $\rho_{\parallel, \perp}^{\pm}(j)$ and $\rho_{\parallel, \perp}^{\pm}(t)$ with allowance for the asymmetric pinning potential. The nature of the behavior of the current and temperature dependence of $\rho_{\parallel, \perp}^{\pm}$ is completely determined by the behavior of the dependences $\nu^{\pm}(j)$ and $\nu^{\pm}(t)$. As follows from formulas (28)–(31), the even resistivities $\rho_{\parallel, \perp}^{+}$ depend only on the even function ν^{+} and, similarly, $\rho_{\parallel, \perp}^{-}$ depend only on the odd function ν^{-} .

The limiting values of the qualitatively similar dependences $\rho_{\parallel}^{+}(j_y)$ and $\rho_{\parallel}^{+}(t)$ corresponding to the TAFF regime of vortex motion transverse to the pinning channels are determined by guided vortex motion along the pinning channels and grow with increasing magnitude of the angle α since in this case the component of the Lorentz force along the pinning channels increases. In the FF regime, as the pinning viscosity becomes isotropic, the contribution to the dependences $\rho_{\parallel}^{+}(j)$ and $\rho_{\parallel}^{+}(t)$ due to vortex motion transverse to the PPP channels becomes substantial, and the limiting values of these dependences are equal to unity (see Figs. 10 and 11).

The main contribution to the even transverse resistivity ρ_{\perp}^{+} is proportional to the factor $\sin(2\alpha)/2$; therefore, the angle most favorable for its observation is near $\alpha = \pi/4$. The current dependence $\rho_{\perp}^{+}(j)$ and the temperature dependence $\rho_{\perp}^{+}(t)$ have their maximum absolute values in the TAFF regime of vortex motion transverse to the PPP channels (the same value is approached if the angle is replaced with its complement in the limit $j \rightarrow 0$ and $t \rightarrow 0$) and go to zero with the onset of the FF regime as a consequence of isotropization of the pinning viscosity. The resistivity ρ_{\perp}^{+} can serve as a measure of the anisotropy of the pinning viscosity since it is determined by the difference of the pinning viscosities transverse to and along the pinning channels (see also Eqs. (28) and (29)).

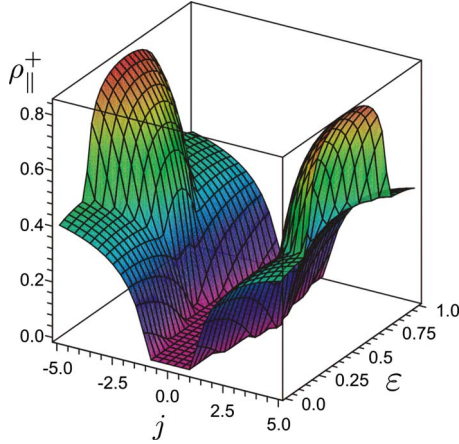


FIG. 11. (Color online) The dependence $\rho_{\parallel}^+(j, \varepsilon)$ for fixed value of the temperature $t_0=0.05$ and angle $\alpha_0=0$.

As can be seen from Figs. 6 and 11 the behavior of the $\rho_{\parallel, \perp}^+(j, \varepsilon)$ resistivities is closely equal to the behavior of the $\nu^+(f, \varepsilon)$. It also follows from Eqs. (28) and (29) that all that have been told about the behavior of the $\nu^+(f, \varepsilon)$ function can be repeated here by analogy. Hence, the steplike appearance of $\rho_{\parallel, \perp}^+(j)$ is a direct consequence of the pinning potential asymmetry. A unique distinction is the influence of the angle α on the $\rho_{\parallel, \perp}^+(j, \varepsilon)$ resistivities by means of internal angular dependence. The internal angular dependence reduces influence of the current on the $\nu^+(j)$ function and causes increasing of the even resistivities along the j axis when α increases.

As was noted above, the odd longitudinal ρ_{\parallel}^- and transverse ρ_{\perp}^- magnetoresistivities arise thanks to the asymmetry of the pinning potential, and therefore their characteristic scale is proportional to ν^- [see Eqs. (30) and (31)]. Therefore, their qualitative form (Figs. 12 and 13) is inherited completely by the behavior of ν^- as a function of the current density, asymmetry parameter, and temperature.

A characteristic peak appears in the $\rho_{\parallel}^-(j)$ dependences in the region of nonlinearity of ν^- as a function of the current density and parameter of asymmetry while in the TAFF and FF regimes of the vortex motion transverse to the pinning

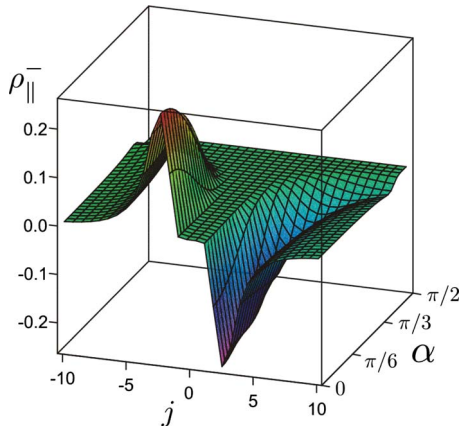


FIG. 12. (Color online) The dependence $\rho_{\parallel}^-(j, \alpha)$ for fixed value of the temperature $t_0=0.05$ and asymmetry parameter $\varepsilon_0=1/3$.

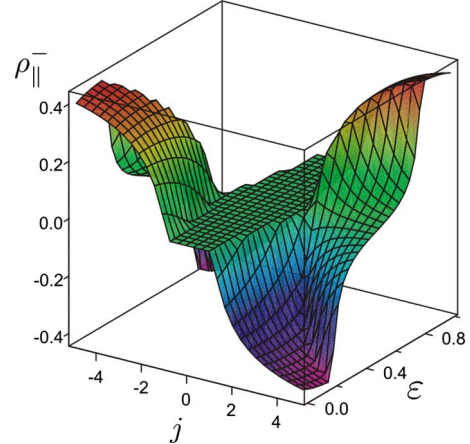


FIG. 13. (Color online) The dependence $\rho_{\parallel}^-(j, \varepsilon)$ for fixed value of the temperature $t_0=0.05$ and angle $\alpha_0=0$.

channels they vanish (Figs. 12 and 13). The temperature behavior of the resistivities ρ_{\perp}^- and ρ_{\parallel}^- is similar to $\nu^-(t)$ behavior (see Figs. 8 and 9). As the main contribution to the odd transverse resistivity ρ_{\perp}^- is proportional to the factor $\sin(2\alpha)/2$, then the most favorable angle for its observation is near $\alpha=\pi/4$. It can be important for experiment that the maximal value of the resistivity ρ_{\perp}^- does not exceed $1/2$, as it follows from Eqs. (29) and (30).

As has been stated above, the resistivity internally depends on the angle α through $f=pj_y=pj \cos \alpha$, and it follows from this that the value of the transport current density, corresponding to maximum of the ρ_{\perp}^- resistivity, can be expressed as

$$j_{max} = \min(j_{cr1}, j_{cr2}) / \cos \alpha. \quad (33)$$

If α tends to $\pi/2$, then j_{max} tends to infinity. This physically means that the Lorentz force, which affects the vortices, is parallel to the pinning channels and cannot drag the vortices across the pinning channels.

It is worth noticing j_{cr1} and j_{cr2} are functions of the asymmetry parameter ε as it was proved in Sec. III A. This explains the fact that, if $\varepsilon \rightarrow 0, 1$, $\rho_{\parallel, \perp}^-$ tends to the steplike or to the bumplike form. It happens because one of the pinning forces tends to infinity.

D. Angular stability of the resistivities in L and T geometries

Let us consider the observed resistivities in the T and L geometries, where the current is directed exactly parallel ($\alpha=0$) or perpendicular ($\alpha=\pi/2$) to the PPP channels. It follows from formulas (28)–(31) that in these limiting cases $\rho_{\perp}^{\pm}=0$, and we obtain for ρ_{\parallel}^+ and ρ_{\parallel}^-

$$\rho_{\parallel, T}^+ = \nu_T^+, \quad \rho_{\parallel, T}^- = \nu_T^- \quad (\alpha=0, \text{ T geometry}), \quad (34)$$

$$\rho_{\parallel, L}^+ = 1, \quad \rho_{\parallel, L}^- = 0 \quad (\alpha=\pi/2, \text{ L geometry}), \quad (35)$$

where longitudinal even $\rho_{\parallel, T}^+$ and odd $\rho_{\parallel, T}^-$ resistivities are due to vortex motion transverse to the PPP channels and are described by the functions $\nu_T^+ = \nu^+(j, t, \varepsilon)$ and $\nu_T^- = \nu^-(j, t, \varepsilon)$, respectively. In the limit $j, t \rightarrow \infty$ we have $\rho_{\parallel, T}^+ = 1$ and $\rho_{\parallel, T}^- = 0$.

The resistivity $\rho_{\parallel,L}^{\pm}$ in the L geometry is equal to unity due to guided vortex motion along the PPP channels, for which pinning is absent. Formulas (34) express simple relations between the observable resistivities $\rho_{\parallel,T}^{\pm}$ and $\rho_{\parallel,L}^{\pm}$ in the T geometry and the form of the functions ν_{\mp}^{\pm} can be reconstructed from their measurements.

Therefore, it makes sense to consider the question of the stability of the measurements in these geometries since the preparation of the samples can lead to small deviations $\delta\alpha$ from the values $\alpha=0, \pi/2$. Here, it should also be borne in mind that besides the resistivities ρ_{\parallel}^{\pm} and ρ_{\perp}^{\pm} assigned by formulas (28) and (31), in the presence of an angle deviation $\delta\alpha$, the resistivities ρ_{\perp}^{\pm} and ρ_{\parallel}^{\pm} , not present in the L and T geometries, also appear. The expansions of $\rho_{\perp,L}^{\pm}$ in α about $\alpha=0$ (in the T geometry) and in $\Delta\alpha=\pi/2-\alpha$ about $\alpha=\pi/2$ (in the L geometry) out to the first nonvanishing terms have the following form:

$$\rho_{\perp,T}^{-} = \nu_{T}^{-}(j)\alpha + o(\alpha^3), \quad (36)$$

$$\rho_{\parallel,T}^{-} = \nu_{T}^{-}(j) - \left(\frac{1}{2} \frac{\partial \nu_{T}^{-}(j)}{\partial j} j + \nu_{T}^{-}(j) \right) \alpha^2 + o(\alpha^3), \quad (37)$$

$$\rho_{\perp,T}^{+} = [\nu_{T}^{+}(j) - 1]\alpha + o(\alpha^3), \quad (38)$$

$$\rho_{\parallel,T}^{+} = \nu_{T}^{+}(j) + \left(1 - \frac{1}{2} \frac{\partial \nu_{T}^{+}(j)}{\partial j} j - \nu_{T}^{+}(j) \right) \alpha^2 + o(\alpha^3), \quad (39)$$

$$\rho_{\perp,L}^{-} = - \left. \frac{\partial \nu^{-}(j)}{\partial j} \right|_{j=0} j(\Delta\alpha)^3 + o((\Delta\alpha)^4), \quad (40)$$

$$\rho_{\parallel,L}^{-} = \left. \frac{\partial \nu^{-}(j)}{\partial j} \right|_{j=0} j(\Delta\alpha)^3 + o((\Delta\alpha)^4), \quad (41)$$

$$\rho_{\perp,L}^{+} = [\nu^{+}(0) - 1](\Delta\alpha) + o((\Delta\alpha)^2), \quad (42)$$

$$\rho_{\parallel,L}^{+} = 1 + [\nu^{+}(0) - 1](\Delta\alpha)^2 + o((\Delta\alpha)^3). \quad (43)$$

Below we will use simple physical arguments in order to estimate a value and to explain all main features of resistivities (36)–(43). The main cause of the presented behavior of the resistivities in the L geometry is extremely small inner dependence ($f \approx j\Delta\alpha$) of the ν^{\pm} functions from the transport current density. Besides, it is easy to see that resistivities $\rho_{\perp,L}^{-}$ and $\rho_{\parallel,L}^{-}$ are close to zero for $t \ll 1$ and $j \ll 1$. This happens because the derivative of ν^{-} is nonzero only in the vicinity of transition from the full guiding regime to the TAFF regime and from the TAFF to the FF regime. The appropriate derivatives and resistivities increase with the temperature and the current density growth until the FF regime occurs. On the other hand, the resistivity $\rho_{\perp,L}^{+}$ in the L geometry varies linearly for small deviations of α and does not depend on the current density. In the same way $\rho_{\parallel,L}^{+}$ does not depend on the small deviation of α and on the current density (see Figs. 10 and 12).

In the T geometry the inner dependence of the ν^{\pm} from the current density is strong ($f \approx j$). The resistivities $\rho_{\parallel,T}^{\pm}$ and $\rho_{\perp,T}^{\pm}$ depend only on ν^{+} and ν^{-} functions and have a weak

angular dependence accordingly. The resistivities $\rho_{\perp,T}^{-}$ and $\rho_{\parallel,T}^{+}$ are proportional to the α deviation. Similarly to foregoing we can conclude that the resistivity $\rho_{\perp,T}^{\pm}$ will be more unstable in comparison with $\rho_{\parallel,T}^{\pm}$ for a small deviation of the angle α from the T geometry (see Figs. 10 and 12).

The relative deviation of the resistivity for a small deviation from the T and L geometries for ρ_{\parallel}^{\pm} is on the order of $\Delta\rho_{\parallel,T}^{\pm}/\rho_{\parallel,T}^{\pm} \sim \alpha^2/\nu(j,t)$ in the T geometry and $\Delta\rho_{\parallel,L}^{\pm}/\rho_{\parallel,L}^{\pm} \sim \Delta\alpha$ in the L geometry. Thus, $\rho_{\parallel,T}^{\pm}$ is the most unstable in the TAFF regime of vortex motion transverse to the pinning channels, where $\nu(j,t) \ll 1$. The physical reason for this behavior is the rapid variation of the angle β from $\alpha=0$ in the T geometry, where the average vortex velocity $v_y=0$, to the angle corresponding to the guiding regime with $v_y \gg v_x$.

The behavior of the resistivities in the L geometry is physically clear from the fact that for $\alpha \approx \pi/2$ the angle β varies hardly at all, i.e., the direction of the velocity vector \mathbf{v} varies only slightly (in contrast to the case of the T geometry) and thermally activated transitions of the vortices through pinning potential barriers play a minor role here.

As was stated above, in an actual experiment small deviations of the angle α from the values $\alpha=0, \pi/2$ corresponding to the L and T geometries are always present. Utilizing experimental measurements of $\rho_{\perp,L}^{\pm}$, these deviations can be found using the following scheme. First, neglecting small quadratic contributions in α to the resistivities $\rho_{\perp,T}^{-}$ and $\rho_{\parallel,T}^{+}$ (in the region where they are stable), it is possible to solve the inverse problem using formulas (37) and (39), i.e., to reconstruct the function ν . Knowing this, from the formulas for the resistivity $\rho_{\perp,L}^{\pm}$, which vanish in the L geometry and are linear for small deviations α , it is possible to find the corresponding value of α deviations. The self-consistency of this scheme is checked by calculating the quadratic corrections in α and $\Delta\alpha$, which should be small relative to the main contribution in the T and L geometries.

E. Weak and strong asymmetries

The definition of weak and strong asymmetries of the pinning potential may be stated as follows. If $f_{p1} \approx f_{p2}$ then this is a weak asymmetry case, and if $f_{p1} \gg f_{p2}$ (or vice versa $f_{p2} \gg f_{p1}$) this corresponds to a strong asymmetry case. The analysis of both limiting cases enables us to compare them and also will lead to some simplifications of the calculations.

Let us discuss first the case when asymmetry of the pinning potential is very small, i.e.,

$$\varepsilon = 1/2 + z, \quad (44)$$

where $z \rightarrow 0$ is the small deviation of the asymmetry parameter from the symmetric case. Substituting Eq. (44) into Eq. (21) we can expand $\nu(f, t, \varepsilon)$ in a Taylor series about small deviation z up to the second-order terms. A convenient result can be presented in the following form:

$$\nu \approx \tilde{\nu} = \tilde{\nu}^{+} + \tilde{\nu}^{-}, \quad (45)$$

where

$$\tilde{\nu}^{\pm} = (f^2 - 4)^2 / [f^2(f^2 - 4) - G] \quad (46)$$

corresponds to the even component of the $\tilde{\nu}$ function expansion into a Taylor series, whereas

$$\tilde{\nu}^- = Wz \quad (47)$$

corresponds to the odd component of $\tilde{\nu}$,

$$G = 16ft\{\cosh[f/(2t)] - \cosh(1/t)\}/\sinh[f/(2t)],$$

and

$$W = 16(4 - f^2)(G + (4 - f^2)\{f \sinh(1/t)/\sinh[f/(2t)] + 2\}/[f(4 - f^2) + G]^2).$$

The insensitivity of the ν^+ function to the small deviation of the ε parameter from 1/2 is the one we could see in Fig. 6, where the $\nu^+(\varepsilon)$ dependence has a maximum at $\varepsilon=1/2$. As a consequence, the resistivities $\rho_{\parallel,\perp}^+$ have similar features in this case (see Figs. 6 and 11). For the $\nu^-(\varepsilon)$ and $\rho_{\parallel,\perp}^-(\varepsilon)$ dependences, $\varepsilon=1/2$ is an inflection point (see Figs. 7 and 13). The $\nu^-(\varepsilon)$ dependence has a maximum in the TAFF regime (see Figs. 7 and 8). This is in a good agreement with the behavior of the $W(f,t)$ dependence, namely, $W=0$ if $f \rightarrow 0$ and if $t \rightarrow \infty$. It follows from this that $W(f)$ also has a maximum in the TAFF regime. The origin of it was discussed in more detail in Sec. III A. Note also that since $\nu^+ \gg \nu^-$ the odd resistivities will be substantially less than even resistivities in this case.

Notice now that the $\tilde{\nu}^+$ function in Eq. (46) is the even function of the external motive force f and coincides with the similar expression given by Eq. (27), which was pointed out earlier in Ref. 13. It is easy also to prove that $\tilde{\nu}^-$ in Eq. (47) is odd with respect to f and z , respectively.

From Eqs. (30), (31), and (47) we can calculate an expression for the asymmetry parameter ε as follows:

$$\varepsilon = 1/2 + \rho_{\parallel,T}^-/W. \quad (48)$$

Note that Eq. (48) can be used for calculating the value of ε from the experimental data in the limit $\alpha \rightarrow 0$ and $\varepsilon \approx 1/2$. The conditions for the most favorable observations of the $\rho_{\parallel,T}$ dependences were discussed in detail in Sec. III C.

In the opposite case, when a pinning force in one direction is considerably larger than a pinning force in another direction, the strong asymmetry arises. Let us consider the case where ε is the small deviation of the asymmetry parameter in the strong asymmetry case (when $f_{cr1}=-1$ and $f_{cr2}=+\infty$). Similarly to the weak asymmetry case, we expand $\nu(f,t,\varepsilon)$ in a Taylor series about a small deviation ε up to the second-order terms,

$$\nu(f,t,\varepsilon) = R_0(f,t) + R_1(f,t)\varepsilon, \quad (49)$$

where

$$R_0 = (f+1)^2/(fX), \quad (50)$$

$$R_1 = C/X^2, \quad (51)$$

with

$$X = 1 + f + 2t \sinh[1/(2t)]\sinh[(1+f)/(2t)]/\sinh[f/(2t)],$$

$$C = (4f^2 + 5f + 2)/f + [(2f^2\{t \cosh[f/(2t)] - t \cosh[(f+2)/2t] + \cosh[1/(2t)]\cosh[(f+1)/(2t)]\} + \sinh[(2+f)/(2t)] \times (1+2f)] - 4t \sinh[1/(2t)]\sinh[(f+1)/(2t)]$$

$$\times (3f+2)]/\sinh[f/(2t)].$$

The R_0 and R_1 dependences are neither even nor odd functions of f . It follows from this that ν^+ and ν^- functions depend on the small deviation ε of the asymmetry parameter and it is possible to present as $\nu^+ = R_0^+ + R_1^+\varepsilon$ and $\nu^- = R_0^- + R_1^-\varepsilon$, where $R_{0,1}^\pm$ are the even and odd parts of the $R_{1,2}$ functions. This fact can help us to extract the ε parameter from the experimental data as

$$\varepsilon = (\rho_{\parallel,T}^+ - R_{0,T}^+)/R_{1,T}^+. \quad (52)$$

Note that Eq. (52) can be used for calculating the value of ε from the experimental data in the limit $\alpha \rightarrow 0$ and $\varepsilon \approx 0$ [in the case $\varepsilon \approx 1$ it is possible to replace ε with 1 and f with $-f$ in formulas (49)–(52)].

As is well known,¹⁴ a difficulty arises in the experimental measurements of the odd resistivity responses since for the cancellation of parasitic thermoelectric voltages the procedure of the ‘‘current averaging’’ is frequently used in the experiments. It leads to the disappearance of the odd resistivities, and we cannot use Eq. (48) for the determination of ε from the experimental measurements. On the other hand, Eq. (52) gives us a possibility to calculate the asymmetry parameter ε only from the even resistivities, which usually can be measured in the experiments with the strong asymmetry pinning potential. But as it follows from Eqs. (49)–(51) and from Fig. 10, ε increasing leads to a larger external current in the experiments for decreasing of the calculation errors.

As has been stated above, the $\nu^+(j)$ dependence has a steplike shape and the $\nu^-(j)$ dependence has a bell-shaped appearance if $\varepsilon \neq 1/2$. From Eq. (44) and from Sec. III A it follows that in the weak asymmetry case the distinction between steps of the $\nu^+(j)$ dependence and the width of the bump of the $\nu^-(j)$ dependence is equal to $\Delta j \approx 8z$. The center of the bump position in the first approximation does not depend on z , i.e., $j_{max} \approx 2$. Similarly, in the strong asymmetry case the distinction between $\nu^+(j)$ steps and the $\nu^-(j)$ bump width is equal to $\Delta j \approx 1/z$ and the bump position also depends on z as $j_{max} \approx 1/z$. These features of the ν^\pm functions lead to the same peculiarities in the resistive responses as it follows from Eqs. (28)–(31).

In summary, we can conclude that in the weak asymmetry case the $\rho_{\parallel,\perp}^+$ resistivities practically do not depend on a small deviation of the asymmetry parameter and tend to their maximum. The absolute values of the $\rho_{\parallel,\perp}^-$ resistivities are proportional to a small deviation of the asymmetry parameter that is very small. On the other hand, in the strong asymmetry case, the absolute value of the even resistivities tends to a minimum; the absolute value of the odd resistivities tends to a maximum and both do not depend on z at the transport current density, which is less than $1/z$ (see Figs. 6 and 7). For this reason it is clear that accurate experimental dc measurements at continuous current may be difficult to perform because in the small asymmetry case the ratchet effect can be suppressed by parasite thermoelectric voltages whereas in a strong asymmetry case the ratchet effect can be noticeable only at strong external transport current that can lead to the thermal smoothing of the observed resistivities.

IV. CONCLUSION

In this work we have proposed exactly solvable two-dimensional model structure for the study of the ratchet effect in superconducting film in the presence of the asymmetric planar pinning potential, which was studied first by experiment in Ref. 7. We have theoretically examined the strongly nonlinear resistive behavior of the two-dimensional vortex system of a superconductor as a function of the transport current density \mathbf{j} , the temperature t , and the angle α between the directions of the current and the PPP channels. The nonlinear (in \mathbf{j}) resistive behavior of the anisotropic vortex ensemble is caused by the presence of anisotropic pinning with asymmetry of the PPP. It is physically obvious that such a pinning at low enough temperatures leads to anisotropy of the vortex dynamics since it is much easier for vortices to move along the pinning channels (the guiding effect in the FF regime, which is linear in the current) than in the perpendicular direction, where it is necessary for them to overcome the pinning potential barriers of the PPP. If under variation of one of the “external” parameters \mathbf{j} , t , and α the intensity of manifestation of the indicated nonlinearity is weakened, then this weakening will lead to an “effective isotropization” of the vortex dynamics, i.e., to a convergence (and in the limit of the absence of nonlinearity, to coincidence) of the directions of the mean velocity vector of the vortices and the Lorentz force.

It is physically clear that the current, temperature, and angle α have qualitatively different effects on the weakening of the pinning and the corresponding transition from anisotropic vortex dynamics to isotropic. With the growth of \mathbf{j} the Lorentz force \mathbf{F}_L grows and the height of the potential barriers decreases, so for $j \geq j_{cr1}$, j_{cr2} (where j_{cr1} , j_{cr2} are the crossover currents of the indicated transitions, whose width grows with the growth of t) these barriers essentially disappear. The quantities j_{cr1} , j_{cr2} depend on α by virtue of the fact that the probability of overcoming the barrier is governed not by the magnitude of the force F_L , but only by its transverse component $F_L \cos \alpha$, so that $j_{cr1,2}(\alpha) = j_{cr1,2}(0)/\cos \alpha$ grows with the growth of α . Since an increase in the temperature t always increases the probability of overcoming the pinning barrier, the transition to isotropization of the vortex dynamics is that much steeper in t , the smaller is the pinning barrier.

In order to analyze theoretically the above-described physical picture of a nonlinear anisotropic resistive response, Secs. II A and III employed a comparatively simple, but at the same time quite realistic, planar model of stochastic pinning. It allows one to reduce the calculations to the evaluation of analytical formulas (28)–(31), which have a simple physical interpretation. A distinguishing feature of this model is the possibility, within the framework of a unified approach, to describe consistently the nonlinear transition from the anisotropic dynamics of a vortex system [for currents $j \ll j_{cr1,2}(\alpha)$ at relatively low temperatures] to isotropic behavior [for currents $j > j_{cr1,2}(\alpha)$ at relatively high temperatures]. In the model under consideration this approach corresponds (for $t > 0$) to a substantially nonlinear crossover from the linear low-temperature TAFF regime to the Ohmic FF regime of the vortex motion.

Proceeding now to a brief description of the main theoretical results, we note here that an analytical representation of the nonlinear resistive response of the investigated system in terms only of elementary functions was possible thanks to the use of a simple but physically realistic model of anisotropic pinning with asymmetric sawtooth PPP (see Sec. III and Fig. 3). The exact solution obtained made it possible to consistently analyze not only the qualitatively clear dynamics of the nonlinear guiding effect, but also the nontrivial question of the interaction of guided vortex motion along PPP channels and the ratchet effect. The most important result in our opinion is the conclusion that the appearance of $\rho_{\parallel,\perp}^-$ magnetoresistivities does not require (as it was in Ref. 12) the Hall effect (see Sec. III). The nonlinear formulas (30) and (31) in agreement with physical intuition (now already nonlinear) clearly demonstrate that the most natural and “sufficient” reason for the relatively large $\rho_{\parallel,\perp}^-$ effects is the asymmetry of the pinning wells. At comparatively low temperatures and weak currents it leads to the realization of a quite intense (over a wide interval of angles around $\alpha = \pi/4$) guided vortex motion along the pinning channels in the TAFF regime, i.e., to the appearance of ρ_{\perp}^+ effects, and at currents $j \approx j_{cr1,2}(\alpha)$, to the appearance of characteristic maxima in the curves of the odd components of the resistivities $\rho_{\parallel,\perp}^-$ (see Sec. III C and Figs. 12 and 13).

An essential result of the present work is also contained in formulas (30) and (31). It is a quantitative description of the interaction of the guiding and ratchet effects, which is valid for all possible values of the asymmetry parameter $0 < \varepsilon < 1$. Formally, this interaction arises as a result of the fact that in the case of anisotropic pinning on asymmetric PPP the force of the overcoming the pinning well [see Eq. (20)], which determines the probability of overcoming the potential barrier (and therewith also determines the magnitude of the component of the vortex velocity perpendicular to the pinning channels), is different in the opposite directions of the x axis. Then arising of the odd resistivities defined by Eqs. (30) and (31) appears only due to the ratchet form of the PPP and to the change of their sign with the current or magnetic field reversals [see Eq. (16)]. Their origin follows from the emergence of a certain equivalence of the xy directions for the case, where a guiding of vortices along the channels of the washboard PPP is realized at $\alpha \neq 0$, $\pi/2$. Note also that for $\alpha = 0$ (T geometry of experiment) Eq. (31) gives in fact the *longitudinal* ratchet signal measured in Ref. 2, whereas in L geometry this signal is zero. At $\alpha \neq 0$, $\pi/2$ the transverse ratchet response also appears [see Eq. (30)]. The key point in the physical interpretation of these formulas is our treatment of the function $\nu(f, t, \varepsilon)$ as the probability of overcoming the potential barriers of the PPP, from which follows an understanding of the evolution of the functions associated with it, ν^{\pm} (see Sec. III), as functions of the magnitude of the current density j , temperature t , and angle α . If, as is usually the case in experiment,⁷ the asymmetry of the pinning potential is sufficiently small ($\varepsilon \approx 1/2$), then formulas (28)–(31) simplify substantially since under these conditions $\nu^- \sim (1/2 + z)$, $z \rightarrow 0$ (see Sec. III E).

In conclusion, it should be noted also that the ratchet effect opens up the possibility for a variety of experimental studies of directed motion of vortices simply by measuring

longitudinal and transverse voltages. Experimental control of amplitude and frequency of the external force, damping, anisotropy parameters, and temperature can be easily provided. In contradistinction with other vortex-based ratchet models, the one presented here allows us to separate the Hall and ratchet voltages, which are similar in their (j, t) behavior but have different origins and magnitudes. Note also that the odd ratchet voltages disappear during the procedure of the current averaging frequently used in experiments^{14,15} for the cancellation of parasitic thermoelectric voltages.

APPENDIX: COMPARISON OF RATCHET AND HALL RESPONSES

In this appendix we discuss in short the inclusion of the Hall effect into the problem under discussion. However, the main goal of this part is to compare the properties of the odd transverse resistivities ρ_{\perp}^{-} , which originate both due to the asymmetry of the washboard PPP and the presence of the Hall effect.

It is easy to show¹² that inclusion of the Hall effect changes the motive force $f = pj \cos \alpha$, given by Eq. (16), into the following form:

$$f(m, n) = mj(n \cos \alpha + \epsilon \sin \alpha), \quad (\text{A1})$$

where $\epsilon \equiv \alpha_H / \eta$ and α_H is the Hall constant. Then it can be shown [see Ref. 12 and Eqs. (39) and (40) in Ref. 16] that

$$\begin{aligned} \rho_{\parallel} &= m(\rho_f D) [(D - \delta^2 v) \sin^2 \alpha + v \cos^2 \alpha], \\ \rho_{\perp} &= m(\rho_f D) [\delta v - D(1 - v) \sin \alpha \cos \alpha], \end{aligned} \quad (\text{A2})$$

where $D \equiv 1 + \delta^2$, $\delta \equiv n\epsilon$, $v = v[F(m, n)] \equiv v(m, n)$, and $\rho_{\parallel, \perp} \equiv \rho_{\parallel, \perp}(m, n)$. From Eqs. (A2) it follows that in the general case [i.e., for $U(x) \neq U(-x)$ as it is supposed in the present paper] it is possible to consider two sets of the ρ measurements. The first one $\rho(n)$ is measured at $m = \text{const}$ and the

field inversion ($\pm n$); in this case $\rho(n) = \rho^{+}(n) + \rho^{-}(n)$, where $\rho^{\pm}(n) = [\rho(+n, m) \pm \rho(-n, m)]/2$. In the second set $\rho(m)$ is measured at $n = \text{const}$ and the current inversion ($\pm m$); then $\rho(m) = \rho^{+}(m) + \rho^{-}(m)$, where $\rho^{\pm}(m) = [\rho(n, +m) \pm \rho(n, -m)]/2$. Reasoning similarly, we define $v^{\pm}(n)$ and $v^{\pm}(m)$. It is important to stress that the procedure of current averaging of the measured voltages leads to zero result for the $\rho^{-}(m)$ resistivities and leaves unchanged the $\rho^{+}(m)$ and $\rho(n)$ resistivities.

Ignoring the analysis of Eqs. (A2) at arbitrary values of α , below we consider for simplicity the case of the T geometry ($\alpha = 0$). In this case it is easy to show the difference between measurements of the odd transverse resistivities which follow from the Hall effect [i.e., for $\rho_{\perp, T}^{-}(n)$] or from an asymmetry of the pinning potential [i.e., for $\rho_{\perp, T}^{-}(m)$]. In this way it follows from Eqs. (A2) that

$$\begin{aligned} \rho_{\parallel, T}^{+}(n) &= m(\rho_f D) v_{T}^{+}(n), \\ \rho_{\perp, T}^{-}(n) &= \delta m(\rho_f D) v_{T}^{+}(n). \end{aligned} \quad (\text{A3})$$

Then from Eqs. (A3) we obtain $\delta = \rho_{\perp, T}^{-}(n) / \rho_{\parallel, T}^{+}(n)$, i.e., we can determine the dimensionless Hall parameter ϵ from the experimentally measured resistivities $\rho_{\perp, T}^{-}(n)$ and $\rho_{\parallel, T}^{+}(n)$. Current averaging does not change this conclusion. However, different situation appears when $\rho_{\perp, T}^{-}(m)$ is calculated. From Eqs. (A2) we obtain that $\rho_{\perp, T}^{-}(m) = \delta m(\rho_f D) v_{T}^{-}(m)$ and the current averaging of $\rho_{\perp, T}^{-}(m)$ gives zero. The δ calculation from the $\rho(m)$ data leads to the specific result $\delta = \rho_{\perp, T}^{-}(m) / \rho_{\parallel, T}^{-}(m)$. In conclusion, carrying out the two sets of experimental magnetoresistivity measurements [$\rho(m)$ and $\rho(n)$] gives us the possibility to separate [due to the different $v^{\pm}(m)$ and $v^{\pm}(n)$ functions in Eqs. (A2) and their different behaviors under the procedure of the current averaging] the Hall and asymmetric odd transverse and longitudinal magnetoresistivity responses.

*shklovskij@univer.kharkov.ua

¹P. Reimann and P. Hänggi, *Appl. Phys. A: Mater. Sci. Process.* **75**, 169 (2002).

²J. E. Villegas, E. M. Gonzalez, M. P. Gonzalez, J. V. Anguita, and J. L. Vicent, *Phys. Rev. B* **71**, 024519 (2005).

³K. Yu, T. W. Heitmann, C. Song, M. P. DeFeo, B. L. T. Plourde, M. B. S. Hesselberth, and P. H. Kes, *Phys. Rev. B* **76**, 220507(R) (2007).

⁴R. Wordenweber, P. Dymashevsky, and V. R. Misko, *Phys. Rev. B* **69**, 184504 (2004).

⁵C.-S. Lee, B. Jankó, I. Derényi, and A.-L. Barabási, *Nature (London)* **400**, 337 (1999).

⁶V. A. Shklovskij, in *Low Temperature Physics: 24th International Conference on Low Temperature Physics—LT24*, AIP Conf. Proc. No. 850 (AIP, New York, 2006), p. 857.

⁷D. D. Morrison and R. M. Rose, *Phys. Rev. Lett.* **25**, 356 (1970); *J. Appl. Phys.* **42**, 2322 (1971).

⁸J. I. Martin, Y. Jaccard, A. Hoffmann, J. Nogues, J. M. George, J. L. Vincent, and Ivan K. Shuller, *J. Appl. Phys.* **84**, 411 (1998).

⁹M. Huth, K. A. Ritley, J. Oster, H. Dosch, and H. Adrian, *Adv. Funct. Mater.* **12**, 333 (2002).

¹⁰A. K. Niessen and C. H. Weijnsfeld, *J. Appl. Phys.* **40**, 384 (1969).

¹¹Y. Mawatari, *Phys. Rev. B* **56**, 3433 (1997).

¹²V. A. Shklovskij, A. K. Soroka, and A. A. Soroka, *Zh. Eksp. Teor. Fiz.* **116**, 2103 (1999) [*JETP* **89**, 1138 (1999)].

¹³O. V. Usatenko and V. A. Shklovskij, *J. Phys. A* **27**, 5043 (1994).

¹⁴O. K. Soroka, Ph.D. thesis, J. Gutenberg University, Mainz, 2004.

¹⁵O. K. Soroka, V. A. Shklovskij, and M. Huth, *Phys. Rev. B* **76**, 014504 (2007).

¹⁶V. A. Shklovskij and O. V. Dobrovolskiy, *Phys. Rev. B* **78**, 104526 (2008).